Nat Hazards (2015) 75:2437–2451
DOI 10.1007/s11069-014-1436-5

ORIGINAL PAPER

Drought severity change in China during 1961–2012 indicated by SPI and SPEI

Wen Wang · Ye Zhu · Rengui Xu · Jintao Liu

Received: 3 April 2014 / Accepted: 12 September 2014 / Published online: 28 September 2014

Abstract Using monthly meteorological observation data at 633 sites in China during 1961–2012, the drought severity change has been investigated in terms of the Standardized Precipitation Index (SPI) and the Standardized Precipitation Evapotranspiration Index (SPEI) with potential evapotranspiration estimated by the Penman–Monteith equation (SPEI_pm). Significant wetting appeared to have occurred in northwestern corner of China (Xinjiang Province), especially in winter. The middle to northeastern Tibetan Plateau also experienced wetting in the last 52 years in general. Significantly, drying occurred in Central China (mostly in the middle Yellow River basin) and southwestern China (Yunnan–Guizhou Plateau) in spring and in autumn. There is no evidence of an increase in drought severity over China taking the whole country into account. On the contrary, the hyper-arid and arid zones got significantly wetter in the last 52 years as indicated by both SPI and SPEI.

Keywords Standardized Precipitation Index · Standardized Precipitation Evapotranspiration Index · Land-surface humidity · Drought

1 Introduction

Drought is among the major natural hazards on the globe, since it affects not only agriculture, but also water supply for various other activities. For instance, using soil moisture data simulated by long-term integrations of a coupled ocean–atmosphere model, Wetherald

W. Wang (✉) · Y. Zhu · R. Xu · J. Liu
State Key Laboratory of Hydrology-Water Resources and Hydraulic Engineering, Hohai University, Nanjing 210098, China
e-mail: w.wang@126.com

W. Wang
Water Resources Section, Faculty of Civil Engineering and Geosciences, Delft University of Technology, P.O. Box 5048, 2600 GA Delft, The Netherlands

and Manabe (1999) showed that soil moisture decreases during most of the year in some semi-arid regions of the subtropical to middle latitudes, such as the southern part of North America, central Asia and the areas around the Mediterranean Sea. Ma and Fu (2006) noticed that the drying trend dominated the eastern part of Northwest China, the central part of North China and Northeast China based on monthly precipitation and monthly mean surface air temperature during 1951–2004. Using a mixture of ground observations, satellite observations, re-analysis data, and modeled data, Dai (2011) showed that there is widespread drying over Africa, East and South Asia, and other areas from 1950 to 2008 in terms of Palmer Drought Severity Index (PDSI), and most of this drying is due to recent warming. Further on, Dai (2013) synthesized observed aridity changes and compared them with model-simulated changes and concluded that the observed global aridity changes up to 2010 are consistent with model predictions, which suggests severe and widespread droughts in the next 30–90 years over many land areas resulting from either decreased precipitation and/or increased evaporation.

At the same time, some other results challenge such kind of link. Zou et al. (2005) calculated PDSI using monthly air temperature and precipitation in China during the period 1951–2003, and found no long-term upward or downward trends in the percentage area of drought in China as a whole, although they argued that there has been increased risk of droughts since the late 1970s as global warming progresses. Bordi et al. (2006) assess drought variability based on NCEP/NCAR and ERA-40 re-analysis data, and found that, ERA-40 re-analysis data unveils a weak "global" trend toward wet conditions, whereas NCEP/NCAR re-analysis suggests the absence of a "global" linear trend in dry/wet conditions. Logan et al. (2010) calculated the Standardized Precipitation Index (SPI) over a portion of the Central United States using monthly precipitation observation data for the 1900–2006 period and found that there are more wetting areas than drying areas in that region. Using daily rain gauge data over Europe, Zolina et al. (2013) found that the duration of wet spells exhibits a statistically significant growth over northern Europe and central European Russia. Van der Schrier et al. (2013) present a new global dataset of monthly self-calibrating Palmer Drought Severity Index (scPDSI) mainly based on Climatic Research Unit (CRU) gridded precipitation and temperature data and satellite-based Global Land Cover Characteristics (GLCC) data, showing that only a few isolated grid squares exhibit trends that are statistically significant, and they conclude that previously published evidence of unusually strong or widespread drying is not supported by their work. Sheffield et al. (2012) argue that previous studies using PDSI algorithm may have overestimated the change in drought over the last 60 years. The algorithm they used, which takes into account changes in available energy, humidity, and wind speed, suggests that there has been little change in drought over the past 60 years. The result of Sheffield et al. (2012) raised a big controversy in hydro-meteorology research community (Romm 2012).

The mentioned inconsistency of detected trends at regional and global scales is raised probably due to the differences in several aspects, including what kind and size of data are used, how the drought is defined, and how the drought index is calculated. As mentioned above, different kinds of data (including meteorological data, streamflow, and/or soil moisture) are used in different studies, and these data are retrieved from different sources (ground observations, satellite observations, re-analysis data, and/or model outputs). Indices used by different researchers for assessing drought varied as well. Besides PDSI and its variants, the Standardized Precipitation Index (SPI) and many others are applied, which may reflect different aspects of water deficiency at land surface.

In the present study, we use ground meteorological observations to investigate the spatial and temporal characteristics of droughts in China. Description about the data and

methods used are given in Sect. 2, results are presented in Sect. 3, and some discussions are made in Sect. 4. Finally, some conclusions are drawn in Sect. 5.

2 Materials and methods

2.1 Data used

Monthly ground-based meteorological observation data are obtained from the China Meteorological Data Sharing Service System (http://cdc.cma.gov.cn.), including precipitation, average temperature, maximum and minimum temperature, relative humidity, sunshine hours, and wind speed. There are over 740 stations in total in the system. Data at sites which are close but have different observational periods (with at least 1 year overlapped) are merged as one data series by the method of regression if their precipitation data during the overlapping period have a correlation coefficient greater than 0.9. In total, 38 sites are merged into 19 sites. After quality checkup, 633 data series (including data at 19 merged sites) with few missing records and observation periods longer than 40 years are used. Among the 633 series, 606 series have full data during the period 1961–2012. All the observation sites are illustrated in Fig. 1. As no data are available in the region of Taiwan, it is not considered in the following study.

2.2 Standardized Precipitation Index (SPI)

Many indices have been developed for measuring the drought severity. Standardized Precipitation Index (SPI) (McKee et al. 1993) is one of the most popular ones, which considers only precipitation. It is based on the probability of recording a given amount of precipitation, and the probabilities are standardized so that an index of zero indicates the median precipitation amount, a negative index drought, and a positive index wet conditions. As the dry or wet conditions become more severe, SPI becomes more negative or positive.

SPI could be computed for different time scales, ranging from 1 month to 24 months, for instance, to capture both short-term and long-term drought.

2.3 Standardized Precipitation Evapotranspiration Index (SPEI)

It has been well recognized by many studies that the marked temperature rise affects the severity of droughts (e.g., Ma and Fu 2006; Rebetez et al. 2006). Therefore, a new drought index—the Standardized Precipitation Evapotranspiration Index (SPEI)—based on precipitation and potential evapotranspiration (PET) is proposed recently by Vicente-Serrano et al. (2010). The procedure to calculate the SPEI index involves the calculation of potential monthly or weekly water deficit/surplus (i.e., monthly or weekly difference between precipitation and PET), the accumulation of deficit/surplus at different time scales, and adjustment to a log-logistic probability distribution. PET is defined as the amount of evaporation that would occur if a sufficient water source was available. There are several methods available for calculating PET. Since the FAO-56 Penman–Monteith (PM) equation (Allen et al. 1998) considers not only temperature, but also the effects of wind speed and relative humidity in the calculation of PET, it is more physically reasonable than the Thornthwaite equation (Thornthwaite 1948) which considers only the

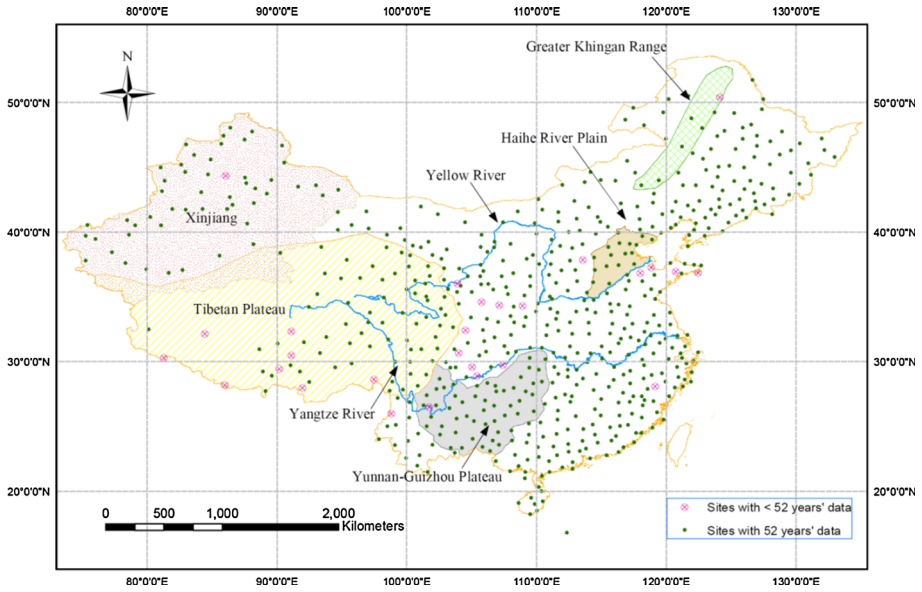

Fig. 1 Locations of the meteorological observation sites

effect of temperature. Therefore, instead of using the Thornthwaite equation as in the original algorithm of SPEI calculation, FAO-PM equation is used to calculate PET in the calculation of SPEI here. The R Package created by Beguería and Vicente-Serrano is used to calculate SPEI, which is available at http://sac.csic.es/spei.

2.4 Mann–Kendall trend test

The Mann–Kendall (MK) test (Mann 1945), a rank-based nonparametric method, is applied in this study to detect the existence of trend.

Under the null hypothesis H_0 that a series $\{x_1,\ldots, x_N\}$ comes from a population where the random variables are independent and identically distributed, the MK test statistic is given by

$$S = \sum_{i=1}^{N-1} \sum_{j=i+1}^{N} \operatorname{sgn}(x_j - x_i), \quad \text{where } \operatorname{sgn}(x_j - x_i) = \begin{cases} +1, & x_j > x_i \\ 0, & x_j = x_i \\ -1, & x_j < x_i \end{cases} \tag{1}$$

To avoid the occurrence of equal values, we may add a small uniformly distributed random value in the interval $(0, \sigma/100)$, where σ is the standard deviation of the series.

Kendall's τ, which measures the strength of the monotonic trend, is estimated by:

$$\tau = \frac{2S}{N(N-1)} \tag{2}$$

The variance of S (σ_s^2) for the situation where there is no ties (i.e., equal values) in the x values, is given by

$$\sigma_s^2 = \frac{1}{18}[N(N-1)(2N+5)] \tag{3}$$

Under the null hypothesis, the quantity z defined in the following equation is approximately standard and normally distributed:

$$z = \begin{cases} (S-1)/\sigma_s & \text{if } S > 0 \\ 0 & \text{if } S = 0 \\ (S+1)/\sigma_s & \text{if } S < 0 \end{cases} \tag{4}$$

At a 0.05 (or 0.1) significance level, the null hypothesis of no trend is rejected if $|z| > 1.96$ (or 1.645).

For a series with given N, we can calculate its σ_s with Eq. (3). At a specified significance level (say, 0.05 or 0.1), we know its corresponding critical value of z, accordingly we can calculate the corresponding statistic S using Eq. (4) and consequently calculate the critical value of Kendall's τ with Eq. (2). For instance, for a series with data size $N = 52$, σ_s is 16059.3, at significance level 0.05 and 0.1, critical values of z are ± 1.96 and ± 1.645 and S are ± 249.4 and ± 209.5, consequently, critical values of τ are approximately equal ± 0.188 and ± 0.158. Based on that, the detected trend could be divided into six zones according to τ, that is as follows: (1) $\tau < -0.188$, indicating significant decrease; (2) $\tau \in [-0.188$ to $-0.158)$, indicating weak decrease; (3) $\tau \in [-0.158$ to $0)$, indicating not significant decrease; (4) $\tau \in [0$–$0.158)$, indicating not significant increase; (5) $\tau \in [0.158$–$0.188)$, indicating weak increase; (6) $\tau \geq 0.188$, indicating significant increase.

For those sites with data size $= M < N$, we assume that the Kendall τ for the period of length N is consistent with the τ for the period of length M with observations. This may exaggerate the trend a little bit, but would not lead to considerable biases.

It is known that the positive serial correlation inflates the variance of the MK statistic S and hence increases the possibility of rejecting the null hypothesis of no trend. By examining the SPI and SPEI time series of different time scales equal or <12 months, we found that the autocorrelation is negligible. Therefore, no preprocessing procedure is applied here.

The Kendall τ of MK trend test for SPI and SPEI time series is spatially interpolated with the method of Inverse Distance Weighted interpolation, so as to make the spatial characteristics viewed intuitively.

3 Results about SPI and SPEI changes

3.1 Spatial and temporal characteristics of SPI

As SPIs of long time scales are basically the accumulation effects of SPIs of short time scales, therefore, to save the space, in the present study, we focus on two time scales, i.e., 1 month and 12 months. As SPI-12 series for different months are similar for each month, only SPI-12 series of December over the 52 years are analyzed. SPI-1 of every month represents standardized precipitation of that month only; SPI-12 of December represents the standardized precipitation totals of December and the previous 11 months. MK trend test was applied to the SPI series with different time scales at each site, and then, the values of Kendall's τ are interpolated over China. The results of SPI-1 and SPI-12 are shown in Figs. 2 and 3.

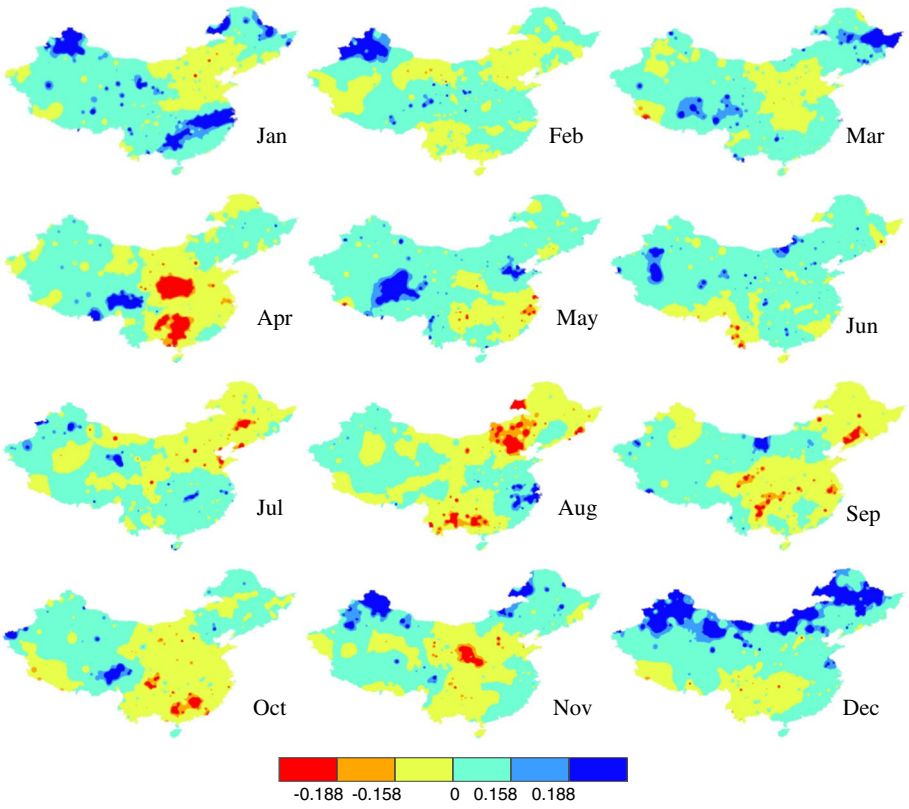

Fig. 2 Distribution of Kendall's τ for 1-month SPI series over China

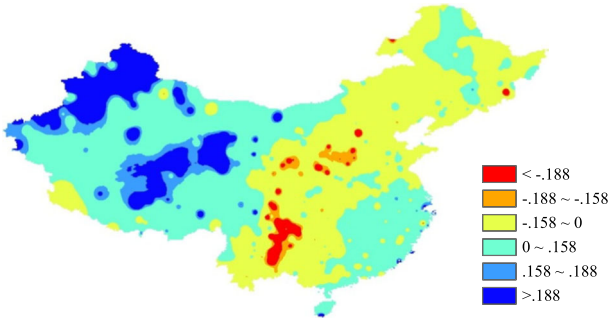

Fig. 3 Spatial distribution of Kendall's τ of 12-month SPI of December

At the 1-month scale, drying or wetting trends can be found in different months and different regions. Significant wetting (i.e., increase of SPI) is observed in southeastern China (mostly in the middle and lower Yangtze River basin) in January, northeastern China in December and March, the middle/eastern Tibetan Plateau in April and May, and especially, the northwestern corner of China (Xinjiang Province) in later autumn to winter

(i.e., November to February). Significant drying (i.e., decrease of SPI) is found in Central China (mostly in the middle Yellow River basin) and the eastern Yunnan–Guizhou Plateau in April, and the region between the Haihe River Plain and the south end of the Greater Khingan Range in August. In summer to early autumn (i.e., June to September), significant drying is also observed in some areas in southwestern China around the Yunnan–Guizhou Plateau. Notably, almost no drying trend around is found anywhere in China in winter and early spring (December to March).

At the 12-month scale, the northwestern half of China generally exhibits a wetting trend, and there are two wetting centers, i.e., Xinjiang Province and the middle to the northeastern Tibetan Plateau. Only some parts in southwestern China (i.e., the Yunnan–Guizhou Plateau) and several small areas in Central and North China (i.e., mostly in the middle Yellow River basin) have significant increase in dryness.

3.2 Spatial and temporal characteristics of SPEI

Similar to the case of SPI, we focus on the SPEI calculated at two time scales, i.e., 1-month and 12-month time scales (referred to as SPEI-1 and SPEI-12) for all sites. MK trend test was applied to the SPEI series with different time scales at each site, and then the values of Kendall's τ are interpolated over China. The results of SPEI-1 and SPEI-12 are shown in Figs. 4 and 5.

At the 1-month scale, months that exhibit significant drying trend (i.e., decrease of SPEI) include August in the Haihe River Plain and the region to the west of the Greater Khingan Range and April in Central China and the Yunnan–Guizhou Plateau. The Yangtze River delta region got drier in April and May. Vast areas in northwestern China experienced significant wetting (i.e., increase of SPEI) from spring to autumn (i.e., April to October). The middle to lower Yangtze River basin got significantly wetter in January and August, so did the Haihe River Plain in May and northeastern China in December.

While the temporal and spatial pattern of SPEI-1 changes are in general in agreement with those of SPI-1 changes, some differences can be found by comparing Figs. 2 and 4. The most remarkable difference is that the significant wetting trend in terms of SPEI is not seen in terms of SPI in Xinjiang during the period from April to October. The drying trend in terms of SPEI in some areas in north Tibet Plateau and northeastern China in February is not observed in terms of SPI either.

At the 12-month scale (Fig. 5, SPEI-12 of December), we can see a clear spatial pattern that Xinjiang and its surrounding regions got wetter (i.e., SPEI increased significantly), whereas some areas in the Central China and the Yunnan–Guizhou Plateau got drier (i.e., SPEI decreased significantly). Comparing the results of SPI-12 and SPEI-12 (in Figs. 3 and 5), we find that while both SPI-12 and SPEI-12 indicate the significant wetting trend in the west part of China, the places they indicated do not match each other exactly.

3.3 SPI and SPEI change in different moisture zones

The spatial–temporal pattern of drought severity change in China is further examined by calculating the average SPI and SPEI in different moisture zones over the 1961–2012 periods. The moisture zone is defined according to land-surface humidity index (HI) defined as the ratio of precipitation P to potential evapotranspiration (PET), that is, HI = P/PET, where PET is calculated with FAO Penman–Monteith formula (Allen et al. 1998).

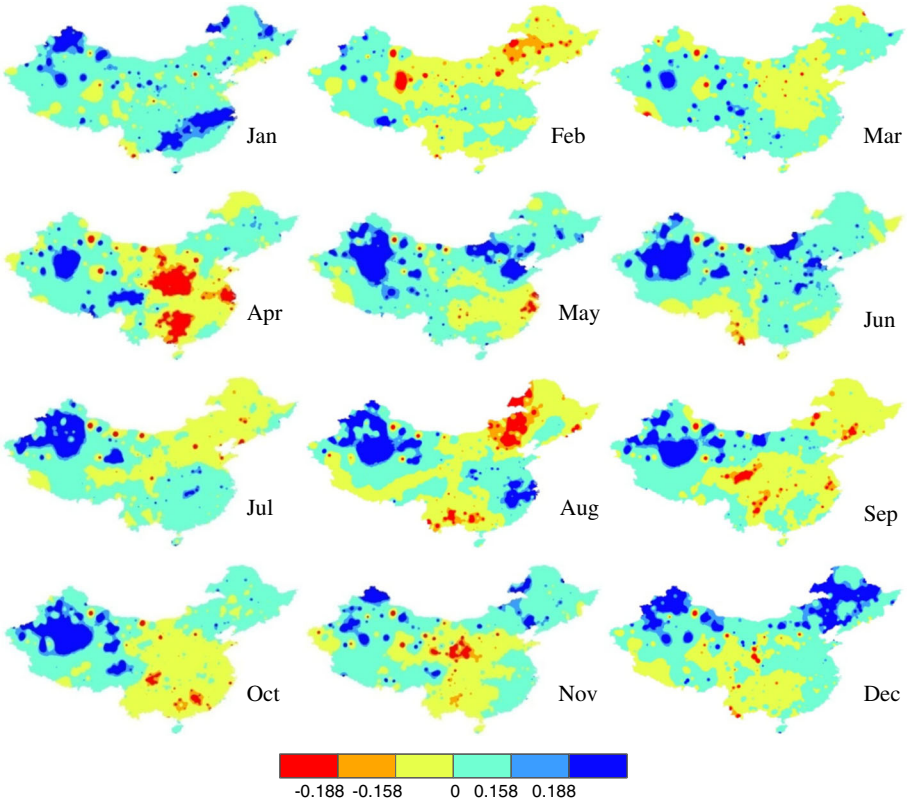

Fig. 4 Distribution of Kendall's τ for 1-month SPEI series over China

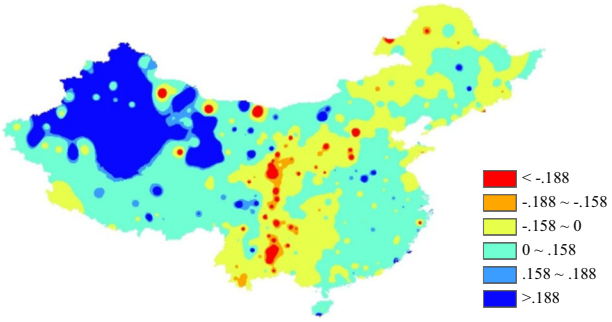

Fig. 5 Spatial distribution of Kendall's τ of 12-month SPEI of December

HI may be calculated at different time scale as SPI and SPEI, but to reflect long-term status of land-surface humidity, it is calculated at the annual time scale here. The annual HI boundaries at 0.05, 0.2, 0.5, and 0.65 were adopted by UNEP/GEMS as the thresholds separating hyper-arid, arid, semi-arid, sub-humid, and humid moisture zones (Hulme et al. 1992). The criteria are modified in the present study by adding a further boundary at

HI = 1. We define the zone with HI > 1 as a hyper-humid zone. Figure 6 shows six moisture zones in terms of the average annual HI all over China during 1961–2012.

We averaged the annual SPI-12 and SPEI-12 of December for each moisture zone over the period 1961–2012. The average SPI-12 and SPEI-12 time series for each moisture zone are shown in Fig. 7, and the MK trend test results for the series are presented in Table 1. From Fig. 7 and Table 1, we see that there is no evidence of the increase in drought severity over China taking the whole country into account. On the contrary, the hyper-arid and arid zones got significantly wetter in the last 52 years in terms of both SPI and SPEI.

4 Discussions

The wetting trend in Xinjiang shown by both SPI and PEI in the present study was noticed more than a decade ago (Hu et al. 2001), and it is believed that the climatic regime there has shifted from warm-dry to warm-wet since the mid-1980s. Such a wetting trend has been confirmed by different drought indices, including precipitation anomaly, PDSI, SPI, and SPEI by the present study and many others (e.g., Ma and Fu 2006; Dai 2013; Zhai et al. 2010).

The wetting trend in southeastern China in winter (mainly in January as shown in Figs. 2 and 4) has been noticed by many studies in the recent decade, and is attributed to the abnormal anticyclone over south Japan transporting warm and humid air from the tropical Pacific to South China (Zhang et al. 2014).

Northeastern China also experienced wetting trend in winter (mainly in December) and early spring (March). That was not reported by earlier studies such as Bordi et al. (2004) who showed that the northern part of eastern China experienced dry conditions more frequently from the 1970s onwards and Ma and Fu (2006) who showed that the central and the southern parts of northeastern China experienced significant drying trend during 1951–2004.

The significant increase in drought severity mostly occurred in Central China and the Yunnan–Guizhou Plateau in terms of both SPI and SPEI according to our study. Some parts in northeastern and northern China also show increased trend of drought in some months, but the extent is less than that shown by some others, such as Dai (2013).

As precipitation is the dominant driving force in the process of drought, SPI has been proven to be a very good indicator of meteorological drought (Keyantash and Dracup 2002) despite its simplicity. Although SPEI is physically sounder than SPI, because SPEI explicitly takes the effects of more meteorological variables (i.e., both precipitation and temperature) regarding drought conditions into account than SPI, the spatial and temporal patterns of drought severity change implicated by SPI and SPEI are basically alike. To explain the reason behind this, first of all, we take two sites in China (Beijing and Urumqi), as examples, plotting their annual precipitation, annual temperature, annual PET with Thornthwaite formula (PET_th), annual PET with Penman–Monteith formula (PET_pm), SPI-12, SPEI-12 calculated with Thornthwaite formula (SPEI_th-12), and SPEI-12 calculated with Penman–Monteith formula (SPEI_pm-12) in Fig. 8.

In the case of Beijing, the mean value of annual precipitation is 556.3 mm with a standard deviation of 160.0 mm, whereas the mean value of annual PET_pm is 1071.7 mm with a standard deviation of 56.1 mm, that is, the coefficient of variation of precipitation (0.288) is much larger than that of PET_pm (0.052). The case of Urumqi (the capital city of Xinjiang Province) is similar to that of Beijing. Because SPEI is calculated based on the difference between precipitation and PET, whereas the range of

Fig. 6 Moisture zones over China in terms of annual HI

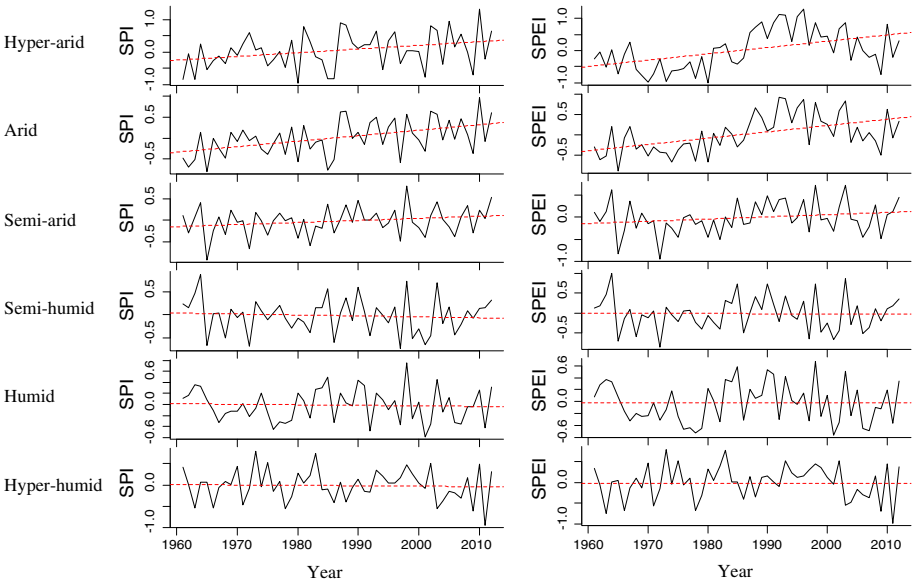

Fig. 7 Average SPI/SPEI time series of different moisture zones over the 1961–2012 period (*Note*: The *dashed line* is the fitted linear regression line)

PET change is much smaller than that of precipitation change, thus the change of SPEI is dominated by the precipitation change. This is clearly indicated by the fact that the absolute values of the correlation between SPEI (in the form of either Penman–Monteith or Thornthwaite) and precipitation is much greater than that between SPEI and temperature (Table 2). Consequently, SPI-12 and SPEI-12 (both SPEI_th-12 and SPEI_pm-12) have basically the same pattern of temporal variations for both Beijing and Urumqi as shown in Fig. 8.

On the other hand, how PET is calculated may affect the SPEI greatly. Since the temperature in Beijing increased significantly, PET_th in Beijing also exhibited significant increase, resulting in the significant decrease in SPEI_th-12 (Fig. 8). However, PET_pm exhibits no significant trend over that last 52 years, therefore, SPEI_pm-12 preserves the

Table 1 MK trend test results for 12-month SPI/SPEI time series of different moisture zones

Moisture zone	SPI		SPEI	
	Tau	*p* value	Tau	*p* value
Hyper-arid	0.204	*0.034*	0.324	*0.001*
Arid	0.302	*0.002*	0.365	*0.000*
Semi-arid	0.107	0.269	0.133	0.167
Semi-humid	−0.051	0.597	−0.006	0.956
Humid	−0.051	0.597	−0.024	0.807
Hyper-humid	−0.045	0.642	0.039	0.687

p values less than 0.05, in italic, indicate that the null hypothesis of no trend could be rejected at the 0.05 significance level

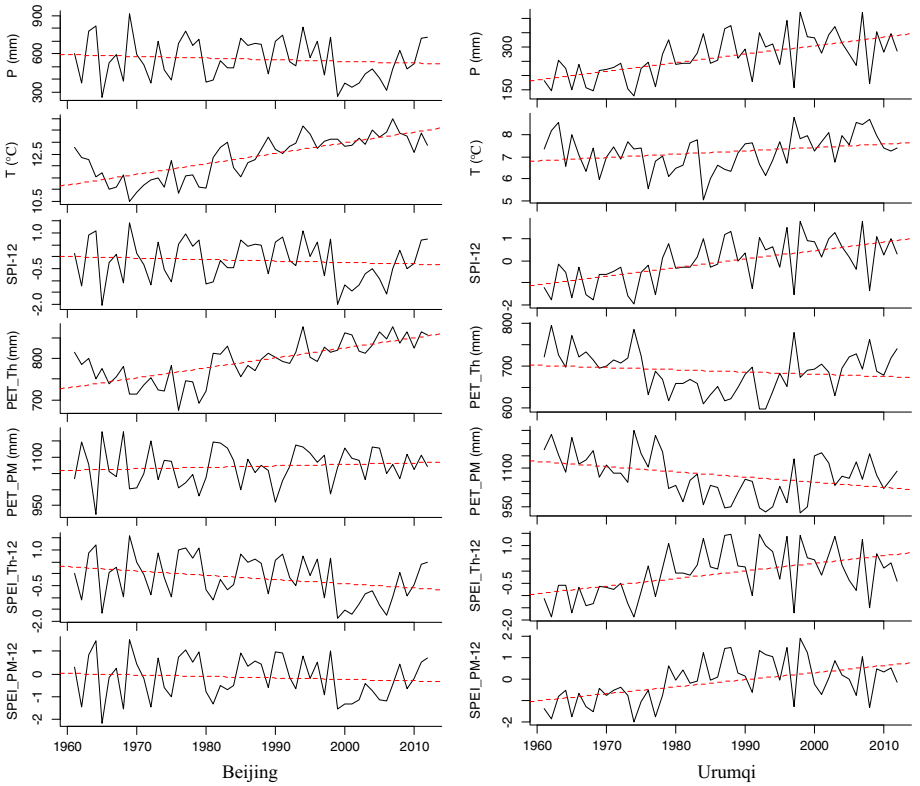

Fig. 8 Annual precipitation, average temperature, PET, SPI and SPEI in Beijing and Urumqi

similar temporal characteristics to SPI in Beijing, i.e., no significant trend. In a recent work of Yu et al. (2014), where droughts over China during the period 1951–2010 are investigated, it is concluded that a significant upward trend of dry conditions occurred in many parts of China, and severe droughts have become more serious since late 1990s for all parts of China. In their study, the calculation of SPEI is based on PET_th. However, by comparing the spatial distribution of Kendall's τ of annual PET_pm (shown in Fig. 9) and annual PET_th (shown in Fig. 10), we see that PET_th indicates an overwhelming

Table 2 Correlation between SPEI-12 and annual precipitation/average temperature

	Urumqi		Beijing	
	SPEI_th	SPEI_pm	SPEI_th	SPEI_pm
Precipitation	0.9456	0.9027	0.9628	0.9714
Temperature	−0.3768	−0.3131	−0.4202	−0.2450

significant increase in PET over China, while significant increases in PET only occur in northwestern part of northeastern China, northeastern part of the Tibetan Plateau and a corner of southwestern China. On the other hand, it is widely recognized now, FAO-56 Penman–Monteith (PM) formula is superior to Thornthwaite formula for potential ET calculation. Therefore, using Thornthwaite formula in the calculation of SPEI may lead to biased assessment of drought change in China.

While the overall difference between SPI and SPEI over China is not great, by comparing the spatial characteristics of SPI and SPEI changes closely, we find that SPEI indicates a larger area of significant wetting that SPI, and the difference between SPI and SPEI is especially obvious in Xinjiang. That is mainly because there are more regions exhibiting decreasing trend in PET than regions exhibiting increasing trend in China, as shown in Fig. 9, and the significant decreasing trend in PET is especially extensive in Xinjiang.

When detecting environment change, several factors may affect the conclusion considerably, i.e., the measures used, the data used, and the time spell of interest.

4.1 Measures used

To measure the drought severity, many indices have been proposed in the last several decades. The use of different indices may lead to considerably different conclusions about drought severity change. It has been noticed that the PDSI tends to show statistically stronger trends than the SPI (e.g., Zhai et al. 2010). That may partly explain the difference in the extent of the areas exhibiting increasing trend of drought severity in northeastern and northern China between our results with that of Dai (2013) which used PDSI as the drought severity indicator. Even for a specific index, different forms may have significant differences, such as SPEI_pm and SPEI_th which use different formula for PET calculation. Although it was claimed by Vicente-Serrano et al. (2010) that the method used to calculate the PET in the drought index calculation is not critical, and the difference between SPEI_pm-12 and SPEI_th-12 for Beijing is not too much by visual inspection in Fig. 8, the Mann–Kendall test shows that there exhibits significant trend for SPEI_th-12 but no trend for SPEI_pm-12 at the 0.05 significance level, which indicates the significant impact of PET calculation on the temporal characteristics of SPEI.

4.2 Data used

It is known that precipitation is the main driver of drought variability, but there are uncertainties in precipitation trends at regional to global scales (Sheffield et al. 2012). Regarding the recent debate over drought change, we can find obvious differences among the data used in different studies. The data used by Sheffield et al. (2012) are mainly from a

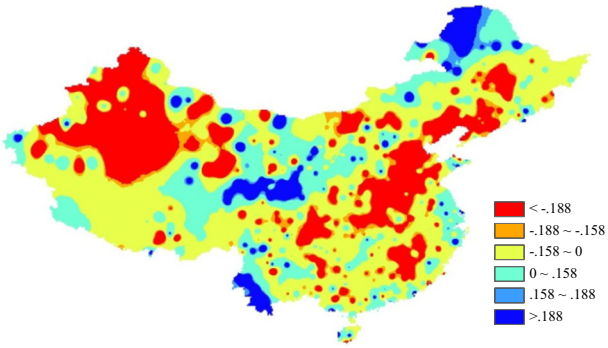

Fig. 9 Spatial distribution of Kendall's τ of annual PET calculated with FAO Penman–Monteith equation

Fig. 10 Spatial distribution of Kendall's τ of annual PET calculated with Thornthwaite equation

global meteorological dataset constructed by combining a suite of global observation-based datasets with the National Centers for Environmental Prediction–National Center for Atmospheric Research (NCEP–NCAR) re-analysis and further processed using down-scaling and disaggregation methods. That is, the data they used are the combination of modeled data and observed data, which are quite different from the data we used in the present study. When investigating global long-term precipitation trends from 1950 to 2010, Dai (2013) used gridded global annual mean observed precipitation data. But comparing our SPI trend detection results (which are based on ground precipitation observations) with his long-term trends, we find that while the general spatial pattern is similar, there are some significant disagreements in some areas which indicate the possible differences in the "*observed*" data used. For instance, the decrease of precipitation described in Dai's research in southeastern China is not observed in our ground observations. Therefore, besides the differences in the way of defining drought and the methods used for assessing the changes by different authors, the discrepancies of the conclusions may mainly be resulted from the differences of the data.

In addition, it should be noted that there may be considerable uncertainty in the detected change in western China, especially in the western Tibetan Plateau, because the density of observation sites there is very low.

4.3 Time spell of interested

Interdecadal low-frequency climate variability and abrupt climate changes have been observed by many researchers. For instance, the North Pacific climate regime shifted in the 1970s marked by a notable transition from the persistent warming (cooling) condition over the central (eastern) North Pacific since the late 1960s toward the opposite condition around the mid-1970s (Nakamura et al. 1997), and the summer rainfall over the middle-lower valley of the Yangtze River and over the whole eastern China experienced a notable regime shift in about 1979 (Gong and Ho 2002). Bordi et al. (2009) showed that the length of data record is found to affect the detected trend of drought and wetness greatly, and the linear trend of wetting or drying in Europe is considerably weaker if the period 1998–2009 is included in the analysis than only considering the period 1949–1997, because of the trend reversal during the last decade. That implies the important effect of the time period considered in the research of change detection, especially for regions that experience nonlinear trends. Differences in the length of data may produce considerable impacts on detected trends.

5 Conclusions

Using monthly meteorological observation data at 633 sites in China during 1961–2012, drought severity change is investigated in terms of the Standardized Precipitation Index (SPI) and the Standardized Precipitation Evapotranspiration Index with potential evapotranspiration estimated using the Penman–Monteith equation (SPEI_pm). Both SPI and SPEI_pm indicate that, significant wetting occurred in northwestern corner of China (Xinjiang Province), especially in winter. The middle to northeastern Tibetan Plateau also experienced wetting in general. Significantly, drying is found in Central China (mostly in the middle Yellow River basin) and southwestern China (Yunnan–Guizhou Plateau) in spring and autumn. In the context of global warming, there is no evidence of an increase in drought severity over China taking the whole country into account. On the contrary, the hyper-arid and arid zones got significantly wetter in the last 52 years in terms of both SPI and SPEI_pm.

Since the coefficient of variation of precipitation is generally much larger than that of potential evapotranspiration (PET) in China, whereas the SPEI_pm is calculated based on the difference between precipitation and PET, the change of SPEI_pm is dominated by precipitation change. Consequently, in general, SPEI_pm is in agreement with SPI which is fully depended on precipitation. However, the way of PET calculation (i.e., using Penman–Monteith equation or using Thornthwaite equation) has a significant impact on the temporal characteristics of SPEI.

When detecting environment change, several factors may affect the conclusion considerably. The discrepancies of the conclusions regarding drought changes reported by different researchers may be resulted from the differences of the data used, their ways of defining drought, and the methods used for assessing the changes.

Acknowledgments Financial supports from Natural Science Foundation of China (41371050), China Science and Technology Support Program (2012BAB03B03) and 111 Project (No. B08048) are gratefully acknowledged.

References

Allen RG, Pereira LS, Raes D, Smith M (1998) Crop evapotranspiration-guidelines for computing crop requirements-FAO irrigation and drainage paper 56. FAO, Rome

Bordi I, Fraedrich K, Jiang JM, Sutera A (2004) Spatio–temporal variability of dry and wet periods in eastern China. Theor Appl Climatol 79:81–91

Bordi I, Fraedrich K, Petitta M, Sutera A (2006) Large-scale assessment of drought variability based on NCEP/NCAR and ERA-40 re-analyses. Water Resour Manag 20:899–915

Bordi I, Fraedrich K, Sutera A (2009) Observed drought and wetness trends in Europe: an update. Hydrol Earth Syst Sci 13:1519–1530

Dai AG (2011) Characteristics and trends in various forms of the Palmer Drought Severity Index during 1900–2008. J Geophys Res. doi:10.1029/2010JD015541

Dai AG (2013) Increasing drought under global warming in observations and models. Nat Clim Change 3:52–58

Gong DY, Ho CH (2002) Shift in the summer rainfall over the Yangtze River valley in the late 1970s. Geophys Res Lett. doi:10.1029/2001GL014523

Hu RJ, Jiang FQ, Fang ZL, Wang YJ (2001) Assessment about the impact of climate change on environment in Xinjiang since recent 50 years. Arid Land Geogr 24(2):97–103 (in Chinese)

Hulme M, Marsh R, Jones PD (1992) Global changes in a humidity index between 1931-60 and 1961-90. Clim Res 2:1–22

Keyantash J, Dracup JA (2002) The quantification of drought: an evaluation of drought indices. Bull Am Meteorol Soc 83:1167–1180

Logan KE, Brunsell NA, Jones AR, Feddema JJ (2010) Assessing spatiotemporal variability of drought in the U.S. central plains. J Arid Environ 74:247–255

Ma ZG, Fu CB (2006) Some evidence of drying trend over northern China from 1951 to 2004. Chin Sci Bull 51:2913–2925

Mann HB (1945) Nonparametric tests against trend. Econometrica 13:245–259

McKee TB, Doesken NJ, Kleist J (1993) The relationship of drought frequency and duration to time scales. Proceedings of the 8th Conference on Applied Climatology. American Meteorological Society Boston, MA, pp 179–183

Nakamura H, Lin G, Yamagata T (1997) Decadal climate variability in the North Pacific during recent decades. Bull Am Meteorol Soc 78:2215–2225

Rebetez M, Mayer H, Dupont O, Schindler D, Gartner K, Kropp JP, Menzel A (2006) Heat and drought 2003 in Europe: a climate synthesis. Ann For Sci 63:569–577

Romm J (2012) Climate change is already worsening droughts in many ways: Nature gets it wrong and right. URL: http://thinkprogress.org/climate/2012/11/20/1194201/climate-change-droughts-nature/

Sheffield J, Wood EF, Roderick ML (2012) Little change in global drought over the past 60 years. Nature 491:435–438

Thornthwaite CW (1948) An approach toward a rational classification of climate. Geogr Rev 38:55–94

Van der Schrier G, Barichivich J, Briffa KR, Jones PD (2013) A scPDSI-based global data set of dry and wet spells for 1901–2009. J Geophys Res Atmos 118:4025–4048

Vicente-Serrano SM, Beguería S, López-Moreno JI (2010) A multiscalar Drought Index Sensitive to Global Warming: the Standardized Precipitation Evapotranspiration Index. J Clim 23:1606–1718

Wetherald RT, Manabe S (1999) Detectability of summer dryness caused by greenhouse warming. Clim Change 43:495–511

Yu MX, Li QF, Hayes MJ, Svoboda MD, Heim RR (2014) Are droughts becoming more frequent or severe in China based on the Standardized Precipitation Evapotranspiration Index: 1951–2010? Int J Climatol 34:545–558

Zhai JQ, Su BD, Krysanova V (2010) Spatial variation and trends in PDSI and SPI indices and their relation to streamflow in 10 large regions of China. J Clim 23:649–663

Zhang L, Zhu X, Fraedrich K, Sielmann F, Zhi X (2014) Interdecadal variability of winter precipitation in Southeast China. Clim Dyn. doi:10.1007/s00382-014-2048-1

Zolina O, Simmer C, Belyaev K, Gulev SK, Koltermann P (2013) Changes in the duration of European wet and dry spells during the last 60 years. J Clim 26:2022–2047

Zou X, Zhai P, Zhang Q (2005) Variations in droughts over China: 1951–2003. Geophy Res Lett 32(4):L04707. doi:10.1029/2004GL021853